AIR INFILTRATION IN BUILDINGS DUE TO WIND PRESSURES INCLUDING SOME NEIGHBORING BODY EFFECTS

W. J. Kelnhofer

Professor, Mechanical Engineering
The Catholic University of America
Department of Mechanical Engineering
Washington, D. C.

ABSTRACT

A procedure is developed for calculating air infiltration rates due to wind pressures on the exterior walls of buildings assuming no chimney and mechanical ventilation effects. Resistance to internal air flow is assumed small. Using the results of wind tunnel tests, calculations are presented showing the significant effects a single neighboring building can have on the infiltration rates. Relative building heights, distance between buildings, and wind direction are varied, and both uniform and shear flows are considered. The results show that depending on the particular two-body configuration, a neighboring building can have a favorable or adverse effect on the infiltration rates.

NOMENCLATURE

A	-	infiltration area
C	-	infiltration (or porosity) constant n-i
C_1	-	Cq_∞^{n-1}
C_s	-	$C_f+C_b+C_\ell+C_r$
C_p	-	pressure coefficient
h_1	-	height of model-A
h_2	-	height of model-B
L	-	distance between model-A and model-B
n	-	exponent
P	-	pressure
ΔP	-	pressure difference (P_o-P_i)
Q	-	infiltration flow rate
q	-	dynamic head ($1/2\ \rho U^2$)
U	-	wind velocity
α	-	wind direction
β	-	ratio of side area to total infiltration area
η	-	ratio of local to total infiltration constant
ξ	-	infiltration number ($Q/CA\ q_\infty$)
ρ	-	mass density of air

SUBSCRIPTS

in	-	into a building
out	-	out of the building
b	-	back
f	-	front
i	-	inside
ℓ	-	left
o	-	outside
r	-	right
∞	-	free stream wind condition

INTRODUCTION AND BACKGROUND

Calculation of energy requirements for heating and cooling is an important part of any building design. It is required for sizing and control of heating and cooling systems, as well as estimating building operation costs. In view of rising fuel costs and the need for energy conservation accurate procedures for calculating energy losses become requisite. Any procedure must consider heat gains and losses due to sources and sinks such as people and equipment, conduction through solid walls of the structure, convection around the structure, radiation through transparant surfaces, and air infiltration into or exfiltration out of the building. The last factor can be of major importance, yet can also be the most uncertain one to accurately calculate.

The most up-to-date procedure for calculating heating and cooling loads [1]* employs the "crack method" for calculating infiltration rates as outlined in the ASHRAE handbook of fundamentals [2]. As will be discussed below, the method states simply that the steady-state volumetric flow rate through a crack or porous opening in a building wall is proportional to the pressure differences across the wall raised to a power as determined for a particular structure. The pressure differences across the wall can be the result of density differences (or the "chimney effect"), operation of mechanical ventilation systems, and wind forces due to the flow of air over and around the building. The actual infiltration distribution around a building depends upon the leakage characteristics of the external walls, and the resistance to internal air movements because of internal walls, floors and other separations.

Relatively little information can be found in the literature regarding pressure differences across walls of actual buildings, and their leakage characteristics. Ref. [3] and [4] give insight into the chimney effect on pressure differences, and Ref. [5] and [6] discuss the combined effect of chimney action and mechanical ventilation. The pressure difference caused by wind is discussed in [7]. These studies show how the total pressure difference is effected by each cause, but more significantly they show that the total pressure difference can be adequately approximated by the superposition of the individual pressure differences due to each cause.

It is clear that strong winds on high buildings can be a major cause of infiltration. Calculation of this wind effect is difficult, and the ASHRAE Procedure [2] is somewhat simplified. Model studies using sharp-edged bluff bodies in wind tunnels show that wind pressure distributions depend on building configuration, structure of the wind, and effects of neighboring bluff bodies such as trees, hills, or other buildings [8,9]. Model studies are much less expensive to conduct than studies with actual buildings, and the data obtained, if proper flow conditions are used, can be reasonably close to what occurs under actual conditions [10].

In 1970, this writer conducted a wind tunnel study to determine the effects that a single neighboring building model can have on the time-averaged wind pressure distribution on a primary building model [11]. Variations were made on the relative heights of the two models, the distance between models, and the wind direction. Both uniform flow and shear flow (to represent boundary layer flow over the earth's surface) were used. It is the purpose of this paper to show how those wind tunnel test results can be used to predict infiltration due to wind pressures alone, i.e., no chimney or mechanical ventilation effects are considered to exist. The assumption is made that internal resistance to air movement is small. Thus, internal pressure under steady state conditions is constant. Results are presented in various ways to show the significant effects of relative building height ratios, distance between buildings, and wind direction on infiltration rates. Comparisons of results for uniform flow and shear flow are made.

CALCULATION PROCEDURE

Air infiltration into a building through porous walls, based on the crack method, is a function of the pressure difference across the walls. Consider a building with porous walls. Under steady-state wind conditions, one can write

$$Q_{net} = Q_{in} - Q_{out} = \int_A C(P_o - Pi)^n dA = 0 \qquad (1)$$

where

Q_{net} = Flow rate through walls (ft^3/min), (m^3/s)

Q_{in} = Flow rate into building (ft^3/min), (m^3/s)

Q_{out} = Flow rate out of building (ft^3/min), (m^3/s)

P_o = Pressure on outside of walls (lb/ft^2), (Pa)

Pi = Pressure on inside of walls (lb/ft^2), (Pa)

C = Infiltration (or porosity) constant ($ft^{2n+1}/min\text{-}lb^n$), ($m^{(2n+1)}/s\text{-}Pa^n$)

n = Flow exponent; between 0.5 and 1

A = Area of Porous Walls (FT^2), (m^2)

The value of C varies according to the type of building construction; it must be assumed or determined experimentally. Reference [2] gives values of C for various type walls, windows, doors, etc. The flow exponent, n, must also be determined by experiment for a certain type "crack". For laminar flow through a crack, n=1, and for turbulent flow, n=0.5.

The internal pressure, P_i, is due to the density variations, mechanical ventilation, and air leakage into and out of the building*. Depending on the internal resistances to flow, P_i can vary throughout building.

It is assumed that the external pressure, P_o, is due to wind motion over and around the building*. Its distribution on a building can be complex. Local

*Numbers in square brackets designate references listed at the end of this paper.

*For no wind, P_o is atmospheric pressure including effects of outside temperature.

time averaged wind pressures on buildings are usually given in terms of a non-dimensional wind pressure coefficient, Cp_∞, defined as

$$Cp = \frac{P_o - P_\infty}{q_\infty} \qquad (2)$$

where

P_∞ = free stream static pressure in the wind

q_∞ = dynamic head of free stream = $1/2 (\rho_\infty U_\infty^2)$ (lb/ft^2), (Pa)

ρ_∞ = density of free stream (lb/ft^3), (kg/m^3)

U_∞ = free stream wind velocity (ft/sec), (m/s)

At a Reynolds number greater than 1000 for incompressible flow over a sharp-edged bluff body, it has been observed that Cp_o remains practically constant [12]. This is due to the fact that the time-averaged flow structure remains invariant, which forms the basis for model studies in building aerodynamics, i.e., wind loading on actual buildings may be predicted from observations of wind loading on building models in wind tunnels at Reynolds numbers several hundred times less than those for actual buildings. Thus, it seems reasonable that Cp_o-values obtained from model studies could be used to advantage in calculating infiltration rates.

If the integrand of Eq.(1) is multiplied and divided by q^n_∞, and P_∞ is added and subtracted inside the parenthesis, Eq. (1) can be arranged as:

$$\frac{Q_{net}}{q_\infty} = \int_A C_1 (Cp_o - Cpi)^n \, dA = 0 \qquad (3)$$

where

$$C_1 = C \, q_\infty^{n-1}$$

$$Cpi = (P_i - P_\infty)/q_\infty$$

When knowledge of Cp_o, C and n is available, a variety of practical infiltration problems can be solved. If Cpi is known, infiltration can be calculated directly. It is the portion of the integral that is positive. (The negative portion is exfiltration, which must be equal in magnitude to infiltration). If Cpi is not known, it can be found by forcing the integral to be zero. A problem of the latter kind is considered here,

As stated previously, it is the purpose of this paper to show wind effects on air infiltration assuming no density and mechanical ventilation effects. A building with small internal resistance to air motion is assumed. Thus, Cpi is constant but unknown. The roof of the building is considered impermeable, and the infiltration constant is considered uniform over a given side. If n is assumed to be unity, Eq.(3) becomes

$$\frac{Q_{net}}{q_\infty} = C_f \int_{A_f} Cp_{o_f} dAf + C_b \int_{A_b} Cp_{o_b} \, dA_b + C_\ell \int_{A_\ell} Cp_{o_\ell} dA_\ell + C_r \int_{A_r} Cp_{o_r} \, dA_r$$

$$-Cpi \, (C_f A_f + C_b A_b + C_\ell A_\ell + C_r A_r) = 0 \qquad (4)$$

The subscripts f,b,ℓ, and r refer to the front, back, left, and right sides of the building respectively. Each integral term is multiplied and divided by the corresponding area of integration, and

$$\frac{Q_{net}}{q_\infty} = C_f A_f \overline{Cp}_f + C_b A_b \overline{Cp}_b + C_\ell A_\ell \overline{Cp}_\ell + C_r A_r \overline{Cp}_r$$

$$-Cpi (C_f A_f + C_b A_b + C_\ell A_\ell + C_r A_r) = 0 \qquad (5)$$

where, for example

$$\overline{Cp}_{o_f} = \frac{1}{A_f} \int_{A_f} Cp_{o_f} \, dA_f \qquad (6)$$

$\overline{Cp}_{o_f}$ is defined as the average wind pressure coefficient on the front side of the building. Equation (5) can be made nondimensional if both sides are divided by $C_s A$ where

$$C_s = C_f + C_b + C_\ell + C_r$$

$$A = A_f + A_b + A_\ell + A_r$$

using

$$\eta_f = \frac{Cf}{Cs}, \text{ etc.}$$

$$\beta_f = \frac{Af}{A}, \text{ etc.}$$

Equation (5) becomes

$$\frac{Q_{net}}{C_s A q_\infty} = \eta_f \beta_f \overline{Cp}_{o_f} + \eta_b \beta_b \overline{Cp}_{o_b} + \eta_\ell \beta_\ell \overline{Cp}_{o_\ell} + \eta_r \beta_r \overline{Cp}_{o_r}$$

$$-Cpi \, (\eta_f \beta_f + \eta_b \beta_b + \eta_\ell \beta_\ell + \eta_r \beta_r) = 0 \qquad (7)$$

Equation (7) can be used to calculate Cpi directly. Then, the infiltration is found by writing Eq.(7) in the form

$$\frac{Q_{net}}{C_s A q_\infty} = \frac{Q_{in}}{C_s A q_\infty} - \frac{Q_{out}}{C_s A q_\infty}$$

$$= \eta_f \beta_f (\overline{Cp}_{o_f} - Cpi) + \eta_b \beta_b (\overline{Cp}_{o_b} - Cpi)$$

$$+ \eta_\ell \beta_\ell (\overline{Cp}_{o_\ell} - Cpi) + \eta_r \beta_r (\overline{Cp}_{o_r} - Cpi) = 0 \qquad (8)$$

The infiltration rate is equal to the positive terms on the right side of Eq.(8) multiplied by particular values of C_s, A, and q_∞.

Thus, to determine Cpi and Qin the average values of the wind pressure coefficients on the sides of the building must be known. The experiment carried out to determine these coefficients including the effects of a neighboring building is described below.

DESCRIPTION OF EXPERIMENT

The experiment was designed to measure time-averaged wind pressure distributions on a sharp-edged bluff body, model-A, as affected by a single neighboring bluff body, model-B. All experiments were done in an open, Goettingen-type wind tunnel at the Institut fur Stromungsmechanik, Technische

Universitat Munich, Germany. Figure (1) is a sketch of the two model arrangement in the wind tunnel.

The dimensions of model-A are shown in Fig.(2) along with the locations of 180 wall pressure taps. The particular configuration of model-A was arbitrary, but it represented a typical modern high rise structure. Model-B had the same cross-sectional dimensions as Model-A, but it was not instrumented. The height of model-A, h_1, was constant, and five different heights of model-B were used so that height ratios of h_2/h_1=0, 0.1, 0.25, 0.5, 0.75, and 1 were tested. With model-B always parallel to model-A, the distance between models, L, was varied to obtain L/h_1=0.125, 0.25, 0.5, 0.75, 1, 1.5, 2, 2.5, 3. 3.5, and 4. For any combination of h_2/h_1 and L/h_1 the wind direction, α, was varied from 0° to 180° in steps of 22.5°. All tests were run at a Reynolds number based on h_1 and U_∞ of approximately 5.2×10^5, which was well above the Reynolds number considered minimum for model testing as discussed above. The pressure taps on Model-A were led individually to a large manometer board. For a given test the entire manometer board was photographed, and later the film was projected on a large screen so that the data could be recorded. Local nondimensional pressure coefficients were calculated according to Eq.(2). Average wind pressure coefficients for a given side of Model-A were obtained through integration as suggested in Eq.(6). Evaluation of the integrals was done numerically using the trapezoidal rule.

The tests included both uniform and shear flow over the two model configuration. Details of the velocity and turbulence intensity profiles in the flows are found in Ref.[13]. With uniform flow Model-A without model-B was about one third submerged in a turbulent boundary layer, and with shear flow, the shear flow thickness was about three times as large as h_1. Results of these tests and application to air infiltration calculations will now be discussed.

TEST RESULTS, APPLICATION AND DISCUSSION

A large number of tests were run to include the combinations of h_2/h_1, L/h_1 and α for both uniform and shear flows. It is clear that not all test results and their application to the calculation of infiltration rates can be presented in this paper. The results presented were selected to show how infiltration rates caused by wind pressures can be calculated, and how these rates may be affected by presence of a single neighboring building.

An appreciation of how a neighboring building can affect the infiltration rate is obtained by an appreciation of how the wind pressure distribution is affected. As an example Fig.(3) is a folded-out plan view showing the $\bar{C}p_o$ - distribution on the sides of model-A standing alone in uniform flow with α=0°. Wind pressures are positive on the front, and suction pressures exist over the back, left, and right sides. The values of $\bar{C}p_o$ for each side are shown. Fig.(4) shows the same results with model-B for L/h_1=0.75 and h_2/h_1=0.5. The effect of model-B on the $\bar{C}p_o$ pattern is considerable. Two regions of positive $\bar{C}p_o$-values and two regions of negative $\bar{C}p_o$ values exist on the front of model A, and $\bar{C}p_o$ values are substantially altered. If the sides of a building represented by model-A were porous, one would certainly expect the infiltration would be strongly affected by the presence of a neighboring building represented by model-B. Similar effects result for shear flow over the two-model combination.

Knowledge of the $\bar{C}p_o$ values on model-A permits one to calculate the infiltration rates according to the previous discussion. First, Cpi can be calculated using Eq. (7). For the application purposes of this paper the following assumptions are made: infiltration can occur only on the front, back, left and right sides; porosity of the walls in uniform over all the building, or, $\eta_f=\eta_b=\eta_\ell=\eta_r$, and C_s = C; any local infiltration or exfiltration is small enough so that the local wind pressure coefficients as obtained from wind tunnel tests are not changed. Cpi from Eq.(7) is

$$Cpi = \beta_f \bar{C}p_{o_f} + \beta_b \bar{C}p_{o_b} + \beta_\ell \bar{C}p_{o_\ell} + \beta_r \bar{C}p_{o_r} \qquad (9)$$

Figures 5 and 6 show the effects of L/h_1 and h_2/h_1 on Cpi for α = 0° with uniform and shear flow respectively. The pattern of effects are the same for both flows, but more pronounced for uniform than for shear flow. A point is seen in each case (L/h_1=2.5 for uniform flow, and L/h_1 = 1.5 for shear flow) where Cpi is approximately the same regardless of h_2/h_1. To the left of the point, strong "sheltering" occurs with larger values of h_2/h_1 pushing Cpi more negative than for smaller values of h_2/h_1. To the right of the point the trend is reversed, but with smaller magnitudes of effects.

The effects of wind direction on Cpi with uniform and shear flow, and L/h_1=0.75 (const.) are shown in Figs. 7 and 8. The general effect with model-B of making Cpi more negative than for model-A alone, is greater for 0° $<\alpha<$ 90° than for 90° $\leq\alpha\leq$ 180°. Again, a greater effect is seen for uniform flow than for shear flow.

The local pressure difference, ΔP, across any wall as caused by wind can be obtained by multiplying the difference between $\bar{C}p_o$ and Cpi by q_∞. The average pressure difference across any wall can be obtained by multiplying the difference between Cp_o for the wall and Cpi by q_∞. Figure [9] shows values of ΔP at one point on the front face of model-A without model-B. The point chosen is on the vertical center line at an elevation of $0.903h_1$. This point corresponds to an instrumented point on an actual 44 story building as reported in Ref. [7]. The data from Ref. [7] is compared to the calculation made in this paper, and the comparison is reasonably good.

The pressure difference across walls vary from point to point in various patterns depending on L/h_1, h_2/h_1, and α. Contour lines of $\Delta Cp(=Cp_o-Cpi)$ can be drawn on a folded out plan view similar to the Cp_o contours shown in Fig.[3 and 4]. Two examples are shown in Fig. 10 and 11. Figure 10 should be compared with Fig.4. The contour pattern of ΔCp shows the regions of driving pressure potential for infiltration (positive ΔCp) and exfiltration (negative ΔCp) as caused by wind. Comparison of Fig. 10 with Fig. 11 shows how these regions can change with a change in the wind from 0° to 67.5°; L/h_1 and h_2/h_1 remained constant.

Values of the nondimensional infiltration were calculated using Eq.(8). With the assumptions stated above, Eq. (8) becomes

$$\begin{aligned}\xi &= \xi_{in} - \xi_{out} \\ &= \beta_f(\bar{C}p_{o_f} - Cpi) + \beta_b(\bar{C}p_{o_b} - Cpi) \\ &+ \beta_\ell(\bar{C}p_o - Cpi) + {}_r(\bar{C}p_{o_r} - Cpi) \qquad (10)\end{aligned}$$

where

$$\xi = \frac{Q}{CAq_\infty}$$

This nondimensional "infiltration number" is useful for purposes of analysis. It can be defined as a local value, an average for one side (or particular portion of a side), or an average value for an entire building. Once the wind pressure distribution is known, ξ can be used for any value of C, A, and q_∞ to calculate infiltration rates due to the wind.

Figures 12 and 13 show effects of L/h_1, h_2/h_1 and α on the infiltration number for air leakage into a building represented by model-A, for both uniform and shear flow. One notes the sheltering effect of model-B or reduction of ξ_{in} for $0° < \alpha < 90°$. At 0° and $L/h_1=4$, the sheltering effect no longer exists with shear flow, whereas it still can be seen for uniform flow. For $90° < \alpha \leq 180°$ model-B stands in the wake of model-A, and the infiltration number can be larger than without model-B. The adverse effect on air leakage is due to the fact that the wake flow of model-A is interrupted by the presence of model-B, and partial recivery of pressure on the downstream side(s) of model-A is hindered. This results in negative pressures of larger magnitude on model-A than those if model-B were not present, but the positive pressures on the upstream side(s) of model-A remain about the same. Similar results have been found by Leutheusser [9].

As mentioned above, the infiltration rate can be calculated from the infiltration number if a value of C is known. For purposes of this paper, a building with plain, 13 inch brick walls will be assumed. Infiltration data for this type wall are found on page 410 of Ref.[2], and it is shown plotted as a function of ΔP in Fig.14. It was shown in Ref. [14] that although the air leakage rate for this type wall is relatively high, it did represent the air leakage characteristics of several tall buildings that underwent actual air leakage tests. The air leakage data shown in Fig.14 has a nonlinear characteristic. However, a straight line drawn through the data is a reasonable approximation for purposes of this paper, so that $Q=69.7\Delta P$ (ft^3/hr) $= 1.16\ \Delta P$ (ft^3/min). Thus, C=1.16 (cfm/min-in.H_2O) for n=1, or, 2.202×10^{-3} (m^3/s-kPa).

The previous results for ξ_{in} were used along with the above value of C to calculate infiltration rates per unit area of building wall (cfm/ft^2)*. Several values of free stream wind velocity were used, and comparisons with uniform and shear flow were made. Figure 15 shows the results for model-A alone. It is a set of reference curves, and can be used for purposes of comparison to see the effects of L/h_1 and h_2/h_1 when model-B is present. The particular shape of the curves in Fig.15 are characteristic to the shape of model-A. If the depth to height to width ratios are changed, it is expected that the shape of the corresponding curves would also change. The effects of L/h_1 for $\alpha = 0°$ and $h_2/h_1 = 0.75$ are shown in Fig.17.

It is easily seen that numerous families of curves could be developed, each family having one change in one parameter. These curves would be very useful for design purposes to show wind effects on infiltration rates.

*This is a common way to present infiltration rates. See Ref.[14] as an example.

The analysis of air infiltration into buildings as caused by wind pressures, and the application of the experimental data to this analysis are based on assumptions that may seem restrictive. These assumptions were made only to show clearly the method of analysis, the distinct effects of a single neighboring building, and the effects of uniform vs. shear flow. Under steady state conditions Eq.(1) can be applied with none of the assumptions made in this paper. The apparent fact that wind, density, and mechanical ventilation effects on the pressure difference across a building wall can be superimposed, makes it clear that P_i in Eq. (1) can include all three effects. The value of n does not have to be unity, and C can vary from position to position on a building. A closed solution to Eq. (1) would, for the general case, not be possible, but a numerical integration would be acceptable.

A more serious restriction toward solution of steady-state infiltration problems needed for energy requirement calculations, is a lack of adequate information on C, n, and wind pressures on buildings. Data such as shown in Fig. 3 and 4 are not available for many basic building configurations. Also, the steady-state analysis may not truly represent actual infiltration rates.

CONCLUSIONS AND RECOMMENDATIONS

The steady state analysis of air infiltration rates caused by wind pressures on buildings as developed in this paper and application of wind tunnel data showing effects of a neighboring building on wind pressures, lead to the following conclusions.

1. Depending on the relative height ratio, distance between buildings, and wind direction, a neighboring building can reduce or increase the infiltration rate per unit area as caused by wind pressures.

2. Neighboring body effects in general are less for shear flow than for uniform flow.

Although the pressure difference across a building wall at one point as calculated in this paper agrees well with a measured pressure difference at a similar point on an actual building, it can hardly be concluded that in general good agreement could be obtained. It is recommended that further comparisons be made where measurements on actual buildings are available. Also, it is recommended that data from other building aerodynamic wind tunnel tests, as well as data from wind loading tests on actual buildings along with the analysis presented in this paper be used to calculate infiltration rates for buildings. Finally, it is recommended that more systematic wind tunnel tests as well as tests on actual buildings be conducted to determine the limits of the aerodynamic and geometric variables associated with the problems of air infiltration.

REFERENCES

1. Procedure for Determining Heating and Cooling Loads for Computerized Energy Calculations, American Society of Heating, Refrigerating and Air-Conditioning Engineers, Inc., 345 E. 47th St., N.Y., N.Y. 10017, 1971.
2. ASHRAE Handbook of Fundamentals, American Society of Heating, Refrigerating and Air-Conditioning Engineers, Inc., 345 E. 47th St., N.Y., N.Y. 10017, 1967.
3. Tamura, G.T. and Wilson, A.G., "Pressure Differences Caused by Chimney Effect on Three High Buildings", ASHRAE Trans., Vol.73, Part II, 1967, pp. 11, 1.1-11.1.10.
4. Barrett, R.E. and Locklin, D.W. "Computer Analysis of Stack Effect in High-Rise Buildings", ASHRAE Trans., Vol.74, Part II, 1968, pp. 155-169.
5. Tamura, G.T. and Wilson, A.G., "Building Pressures caused by Chimney Action and Mechanical Ventilation", ASHRAE Trans., Vol.73, Part II, 1967, pp. 11.2.1 - 11.2.9
6. Tamura, G.T. and Wilson, A.G., "Pressure Differences for à Nine-Story Building as a Result of Chimney Effect and Ventilation System Operation", ASHRAE Trans., Vol. 72, Part I, 1966, pp. 180-189.
7. Tamura, G.T. and Wilson, A.G., "Pressure Differences caused by Wind on Two Tall Buildings", ASHRAE Trans., Vol. 74, Part II, 1968, pp.170-181.
8. Cermak, J.R., "Determination of Wind Loading on Structural Models in Wind Tunnel Simulated Winds", Proceedings of Symposium on Wind Effects on High Rise Buildings, Northwestern University, Evanston, Illinois, March 23, 1970.
9. Leutheusser, H.J., "Static Wind Loading of Grouped Buildings", Proceedings of the Third International Conference on Wind Effects on Buildings and Structures, Tokyo, Japan, September 6-9, 1971, pp.211-219.
10. Standen, N.M., Dalgliesh, S.A., and Templin, R.J., "A Wind Tunnel and Full-Scale Study of Turbulent Wind Pressures on a Tall Building", Proceedings of the Third International Conference on Wind Effects on Buildings and Structures, Tokyo, Japan, September 6-9, 1971, pp. 199-209.
11. Kelnhofer, W.J., "Stromungstechnische Untersuchung Uber den Einfluss eines parallel stehenden Nachbargebaudes auf die Windbelastung eines Gebaudemodells mit rechteckigen Grundiss und Flachdach", Bericht Nr. 70/4a, 70/4b, 70/4-c, Institut fur Stromungsmechanik, Technische Universitat, Munich, Germany, 1970.
12. Leutheusser, H.J. and Baines, W.D., "Similtude Problems in Buildings Aerodynamics", Journal of the Hydraulics Division, ASCE, Vol. 93, No. HY3, May 1967, pp. 35-49.
13. Kelnhofer, W.J., "Neighboring Body Effects on Bluff Body Form Drag", Proceedings of the thirteenth Midwestern Mechanics Conference, University of Pittsburg, Pittsburg, Pa., August 13-15, 1973.
14. Shaw, C.Y., Sander, D.M., and Tamura, G.T., "Air Leakage Measurements of the Exterior Walls of Tall Buildings",ASHRAE Trans., Vol.79, Part II, 1973, pp.40-48.

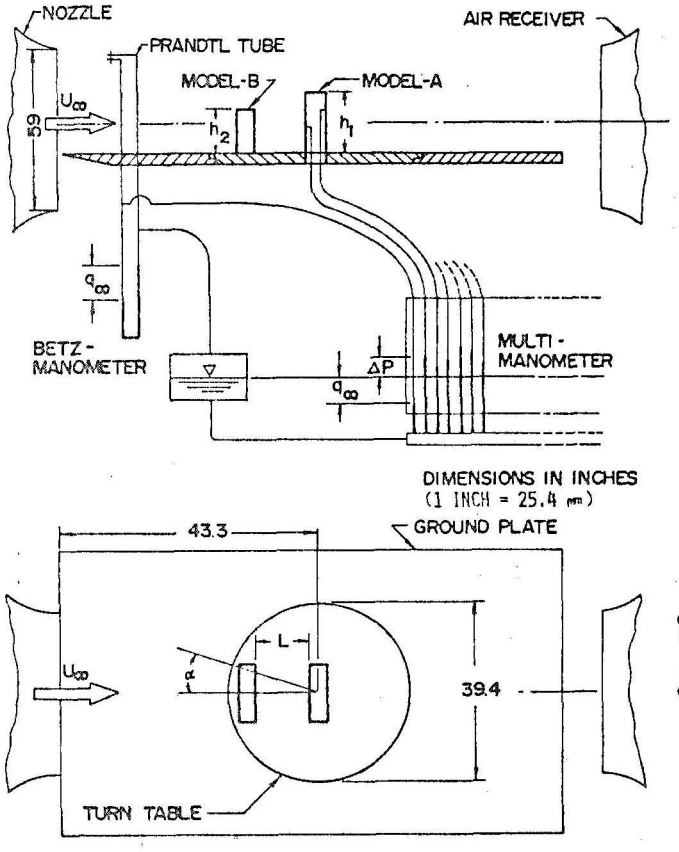

FIG. 1 WIND TUNNEL ARRANGEMENT

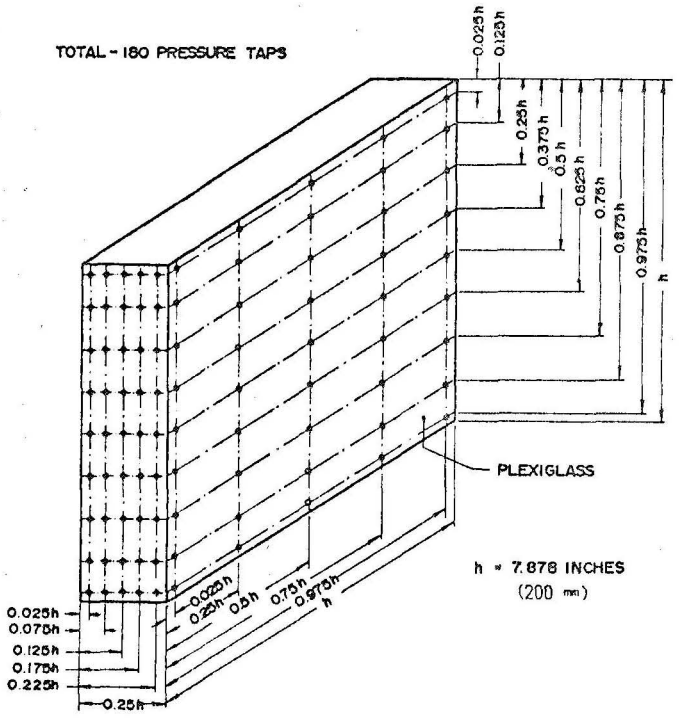

FIG. 2 MODEL-A WITH PRESSURE TAP LOCATIONS

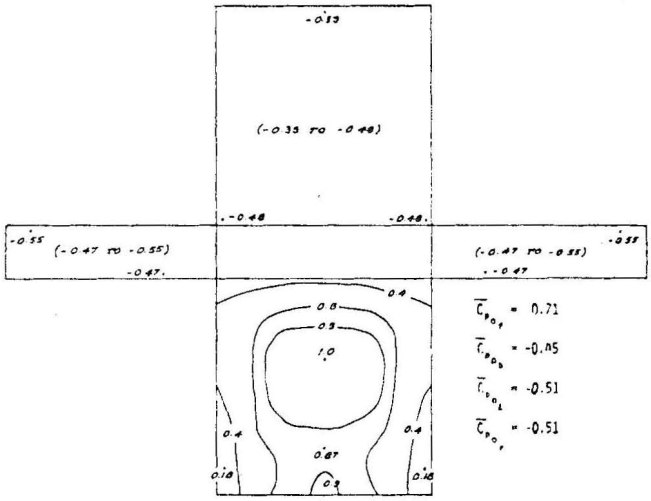

FIG. 3 LINES OF CONSTANT C_{p_o} ON MODEL–A; $\alpha = 0^o$, $L/h_1 = 0$, $h_2/h_1 = 0$

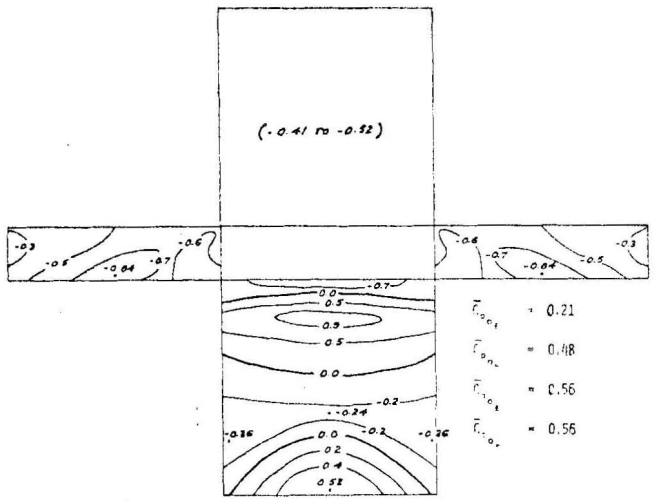

FIG. 4 LINES OF CONSTANT C_{p_o} ON MODEL–A; $\alpha = 0^o$, $L/h_1 = 0.75$, $h_2/h_1 = 0.5$

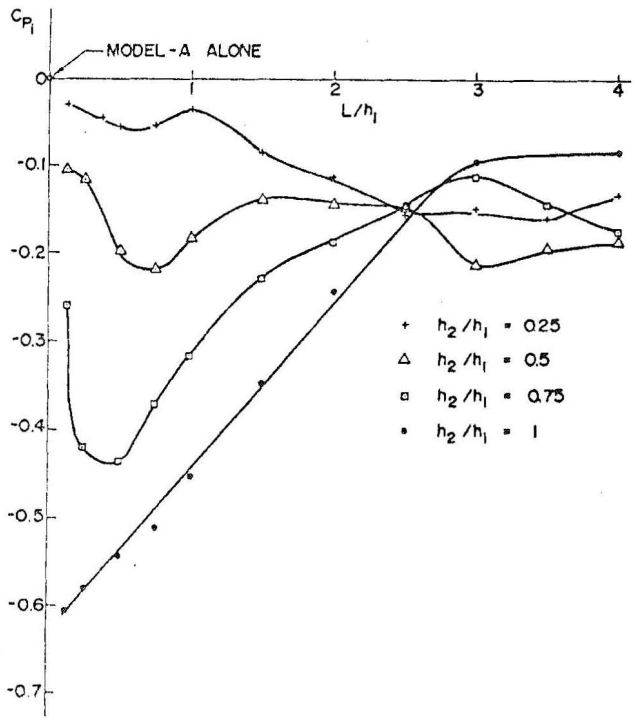

FIG. 5 Cpi FOR MODEL–A–UNIFORM FLOW; $\alpha = 0^o$

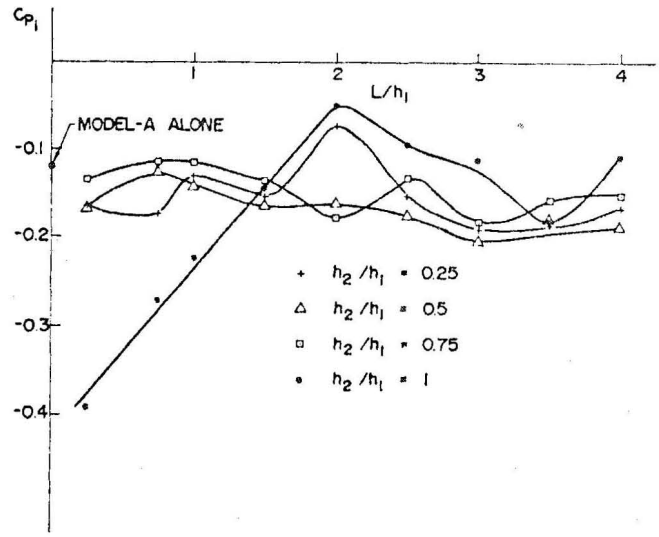

FIG. 6 Cpi FOR MODEL–A–SHEAR FLOW; $\alpha = 0^o$

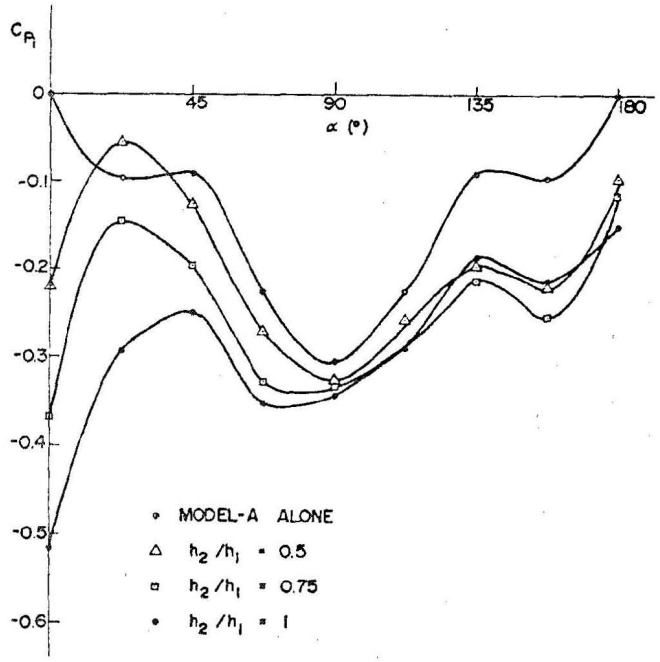

FIG. 7 Cpi FOR MODEL–A–UNIFORM FLOW; $L/h_1 = 0.75$

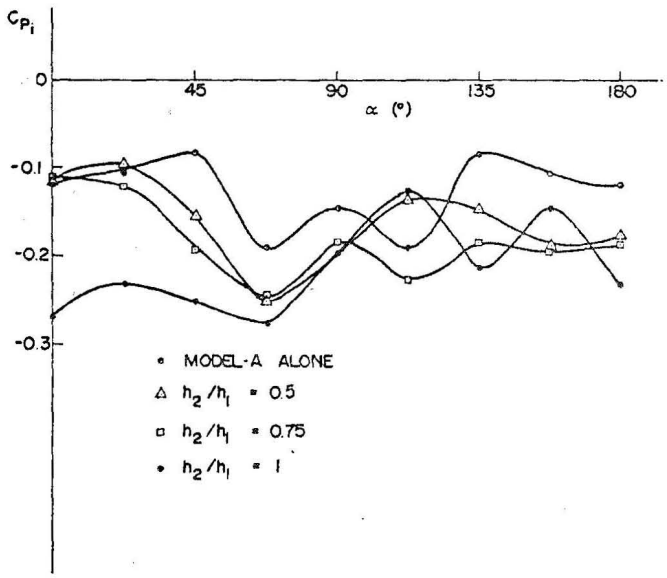

FIG. 8 Cpi FOR MODEL–A–SHEAR FLOW; $L/h_1 = 0.75$

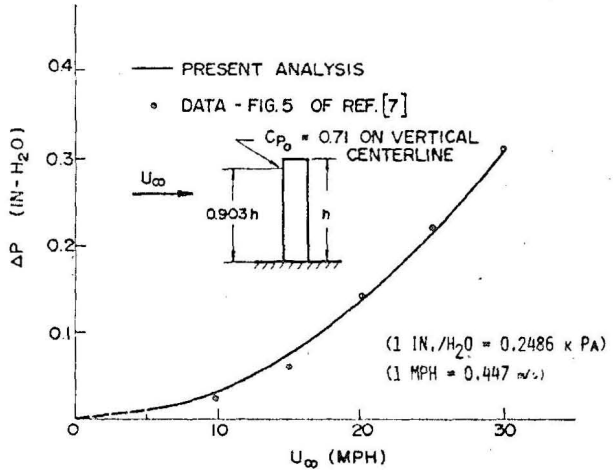

FIG. 9 PRESSURE DIFFERENCE ACROSS FRONT OF MODEL–A ALONE, UNIFORM FLOW; $\alpha = 0^o$

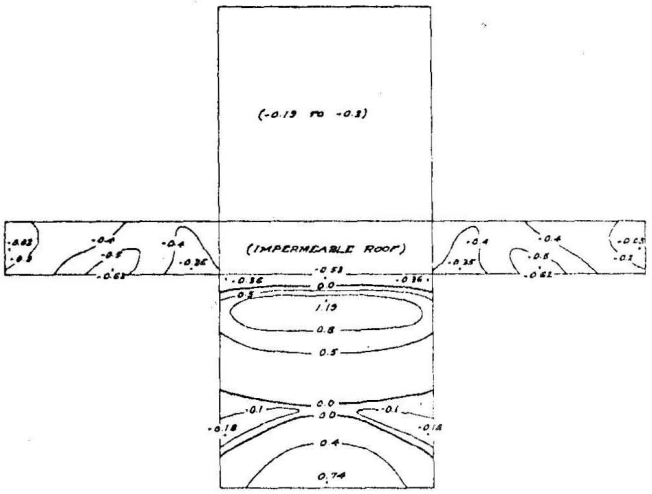

FIG. 10 LINES OF CONSTANT ΔCp ON MODEL–A, UNIFORM; Cpi = 0.22, $\alpha = 0^o$, $L/h_1 = 0.75$, $h_2/h_1 = 0.5$

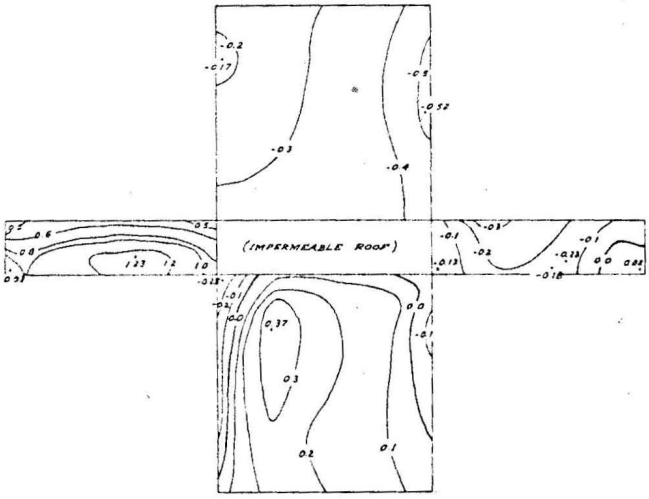

FIG. 11 LINES OF CONSTANT ΔCp ON MODEL–A, UNIFORM FLOW; Cpi = 0.22, $\alpha = 0^{\circ}$, $L/h_1 = 0.75$, $h_2/h_1 = 0.5$

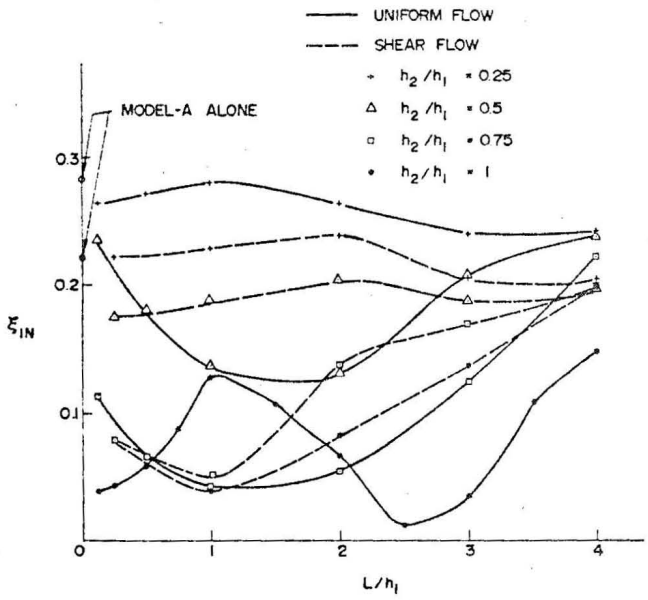

FIG. 12 INFILTRATION NUMBER FOR MODEL–A, $\alpha = 0^{\circ}$

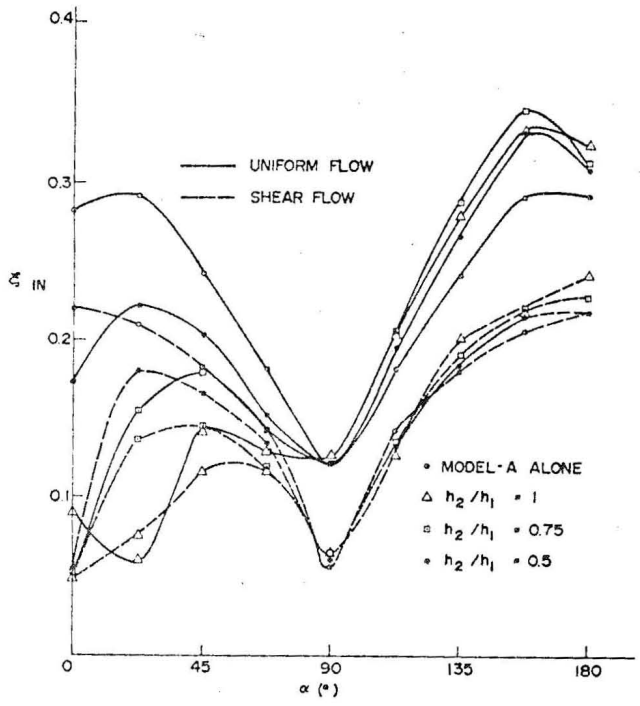

FIG. 13 INFILTRATION NUMBER FOR MODEL–A, $L/h_1 = 0.75$

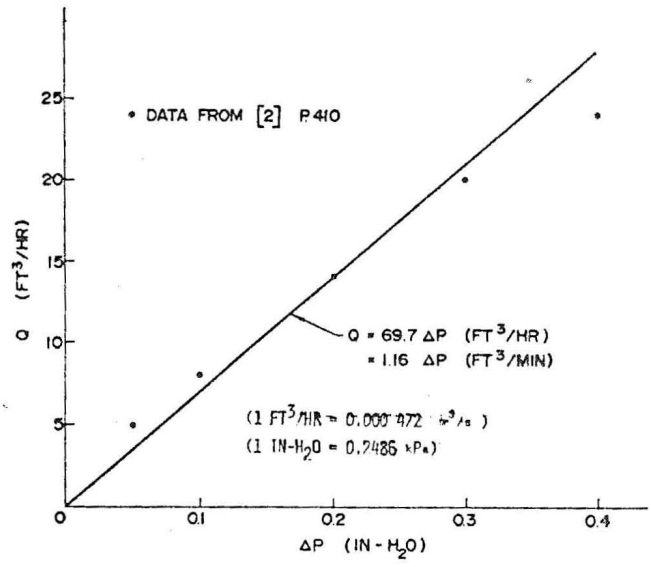

FIG. 14 INFILTRATION RATE FOR 13 INCH THICK PLAIN BRICK WALL

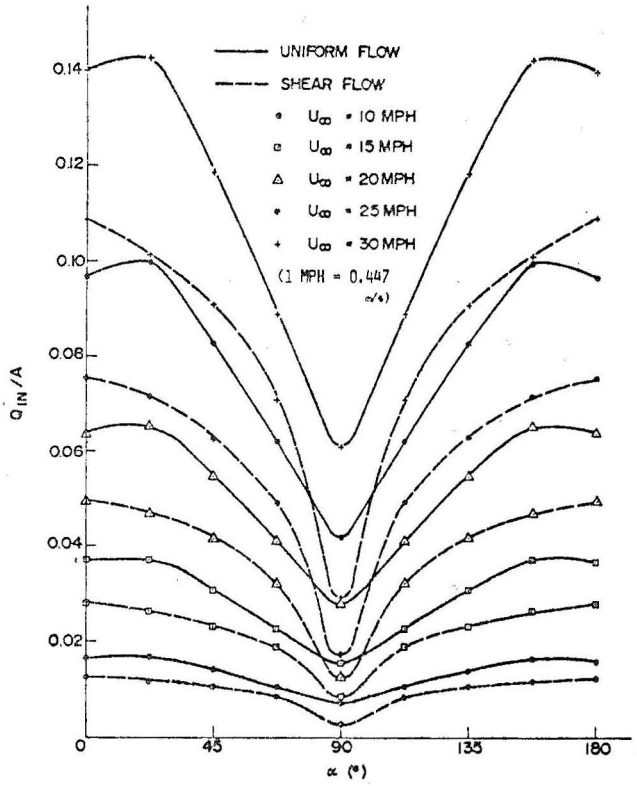

FIG. 15 INFILTRATION RATE PER UNIT AREA – MODEL–A ALONE

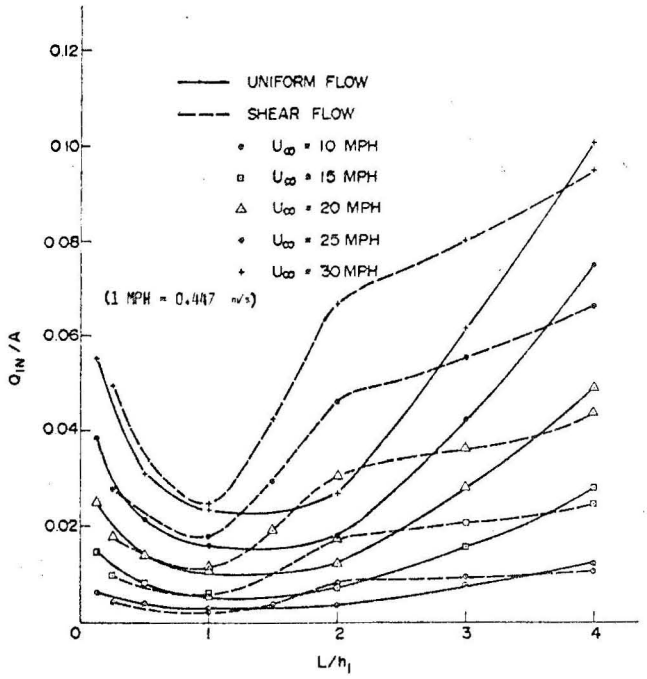

FIG. 16 INFILTRATION RATE PER UNIT AREA WITH MODEL–B, $\alpha = 0^0$, $h_2/h_1 = 0.75$

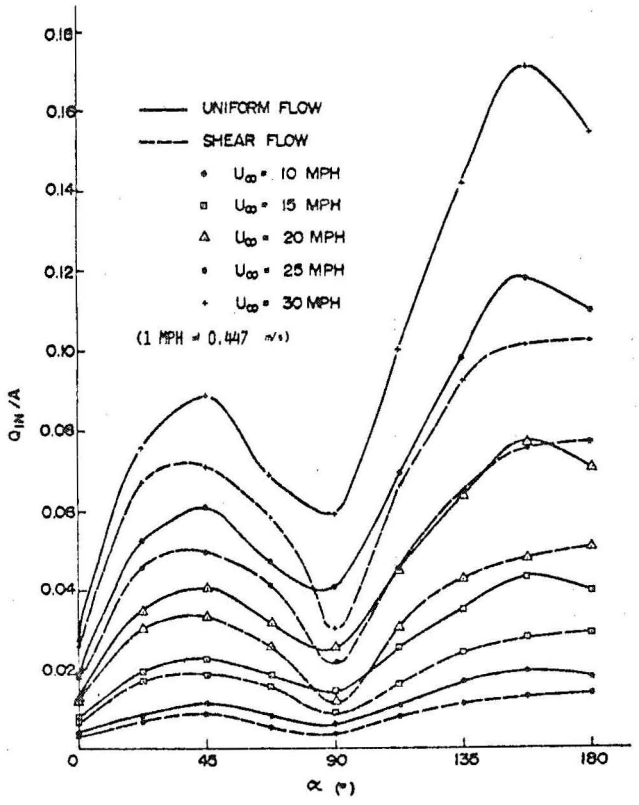

FIG. 17 INFILTRATION RATE PER UNIT AREA WITH MODEL–B; $L/h_1 = 0.75$, $h_2/h_1 = 0.75$